EUROPEAN FUSION DEVELOPMENT AGREEMENT

EFDA–JET–CP(04)03-12

C D Challis and JET EFDA Contributors

The Use of Internal Transport Barriers in Tokamak Plasmas

The Use of Internal Transport Barriers in Tokamak Plasmas

C D Challis and JET EFDA Contributors*

1

EURATOM/UKAEA Fusion Association, Culham Science Centre, Abingdon, Oxon, OX14 3DB, UK
** See annex of J. Pamela et al, "Overview of Recent JET Results and Future Perspectives", Fusion Energy 2002 (Proc. 19th IAEA Fusion Energy Conference, Lyon (2002).*

Preprint of Paper to be submitted for publication in Proceedings of the
31st EPS Conference,
(London, UK. 28th June - 2nd July 2004)

ABSTRACT

Internal transport barriers can provide high tokamak confinement at modest plasma current. This is desirable for operation with most of the current driven non-inductively by the bootstrap mechanism, as currently envisaged for steady state power plants. Maintaining such plasmas in steady conditions with high plasma purity is challenging, however, due to MHD instabilities and impurity transport effects. Significant progress has been made in the control of ITB plasmas: the pressure profile has been varied using the barrier location; q-profile modification has been achieved with non-inductive current drive; and means have been found to affect density peaking and impurity accumulation. All these features are, to some extent, interdependent and must be integrated self-consistently to demonstrate a sound basis for extrapolation to future devices.

1. INTRODUCTION

The goal of realising a steady state tokamak fusion power plant has motivated intensive experimental investigation of plasma regimes suited to fully non-inductive operation at high fusion power and fusion gain (Q ≡ fusion power/input power). The aim to avoid inductive current drive as far as possible, except transiently, follows from the desirability of continuous power generation and the minimisation of the effects of pulse cycling on the tokamak structure. The goal of economical operation places limitations on the amount of external current drive that can be used due to the need to avoid excessive recirculating power. To attempt a precise optimisation from an economic point of view would be premature, but the following considerations have motivated the direction of many experimental investigations in recent years.

Improved plasma energy confinement is desirable compared with the ELMy H mode regime, which serves as the inductive reference regime for many existing tokamaks and, prospectively, ITER [1]. The H mode regime is characterised by a pressure pedestal at the plasma edge and ELMs (edge localised modes) are MHD instabilities that can intermittently degrade the edge pressure gradient to provide quasi steady conditions. The observation that energy confinement improves with increasing plasma current in H mode [2] allows operation at high fusion yield to be envisaged. However, in conventional aspect ratio tokamaks the plasma current required in this regime would place substantial demands on the non-inductive current drive systems, thus making it difficult to achieve high Q in steady state [3]. If a confinement enhancement can be achieved compared with an ELMy H mode, so that $H_H > 1$ ($H_H \equiv$ energy confinement time/ELMy H mode confinement scaling), then an equivalent fusion yield might be obtained with a relatively smaller plasma current. An additional benefit is that the fraction of the current provided by the self-generated non-inductive bootstrap current (the bootstrap fraction) in a tokamak plasma increases with poloidal β ($\beta_P \equiv 2\mu_0 \langle p \rangle / \langle B_{Pa} \rangle^2$, where $\langle p \rangle$ is the averaged plasma pressure and $\langle B_{Pa} \rangle$ is the averaged poloidal field strength at the plasma boundary due to the plasma current), and becomes dominant in the range $\varepsilon^{0.5}\beta_P > 1$ (where ε is the inverse aspect ratio) [4,5]. Thus reducing the plasma current required to achieve a given plasma pressure from a transport point of view can dramatically reduce the

external non-inductive current drive requirement, which is given by the difference between the diminishing total current and the increasing bootstrap current. Increasing H_H through the edge pressure pedestal has the disadvantage that a large fraction of the bootstrap current would be situated in the plasma periphery, which could destabilise MHD kink modes, and the steep edge pressure gradients would have to be compatible with safe operation of the tokamak divertor. Consequently, considerable effort has been devoted to the development of plasma scenarios with improved core confinement.
Increasing the ratio of the plasma pressure to the plasma current is in any event challenging from the point of view of plasma stability. A figure of merit for this is the normalised
β ($\beta_N \equiv 100\beta_T aB/I_{MA}$, where a is the minor radius at the plasma boundary, B is the toroidal magnetic field strength in T and I_{MA} is the plasma current in MA and $\beta_T \equiv 2\mu_0 <p>/B^2$). In general β_N rises with the ratio of the plasma pressure to the plasma current and becomes progressively more difficult to maintain in steady state. Taking the ELMy H mode confinement scaling IPB98(y,2) [2] we can express the β_N in terms of H_H, neglecting fast particle pressure, to give:

$$\beta_N = H_H \, P_{loss,\,MW}^{0.31} \left(\frac{0.477 \, M_{AMU}^{0.19} \, n_{19}^{0.41}}{I_{MA}^{0.07} B^{0.85} R^{0.03} \varepsilon^{0.42} \kappa^{0.22}} \right)$$

where $P_{loss,MW}$ is the loss power in MW, M_{AMU} is the main ion mass, n_{19} is the average plasma density in $10^{19} m^{-3}$, R is the plasma major radius and κ is the plasma elongation. Given that high plasma density is required for high fusion yield and the toroidal magnetic field strength is limited by engineering constraints it can be seen that, for a given device, the value of β_N must be raised together with H_H if the loss power is to be maintained. In a high Q device, the loss power is dominated by α-particle heating and so any significant reduction in the loss power represents a direct reduction in the fusion power output. In the case of ITER, taking typical plasma conditions, loss power of 150 MW, density of 1.1×10^{20} m^{-3} and plasma current of 15 MA [1], we can see that:

$$\beta_N \approx 2H_H$$

Thus, inductive scenarios for ITER are envisaged with $H_H \approx 1$ and
$\beta_N \approx 2$, whereas non-inductive scenarios are being considered at reduced current ($\approx$ 9 MA) with H_H $\approx$ 1.5 and $\beta_N \approx 2.9$ [1]. The potential benefits of achieving even higher values of β_N can be seen from power plant studies such as ARIES-RS [6].

The concept of a fully non-inductive high Q tokamak that generates most of its plasma current using the bootstrap effect through simultaneously high β_N, β_P and H_H, has become known as the Advanced Tokamak. A candidate regime has been obtained in present devices where regions in the plasma interior exhibit enhanced thermal insulation compared with an ELMy H mode in equivalent conditions. These regions are known as Internal Transport Barriers (ITBs). An early example of the use of an internal transport barrier to achieve high fusion performance was the Pellet Enhanced Performance (PEP) regime reported at JET [7]. In these cases, small pellets of frozen deuterium

were injected into the plasma at high velocity to generate a high core density. Subsequent heating by energetic neutral beam injection (NBI) or ion cyclotron resonance wave heating (ICRH) resulted in a high core pressure due to the reduced energy and particle transport. It was noted that this was associated with a region of negative, or reversed, magnetic shear ($s \equiv r/q(dq/dr)$ where r is the minor radius and q is the safety factor, which equals rB/RB_P in the circular cross-section, large aspect ratio approximation). ITBs without pellet injection were observed at JT-60U [8] in what has been called the high β_P mode. In this case intense NBI was applied to low density plasmas, which spontaneously generated very steep gradients in the ion temperature and density profiles. In these cases a link between the barrier location and the $q = 3$ surface was indicated. Experimenters at DIII-D and TFTR reported ITBs in plasmas with negative magnetic shear generated by NBI heating early in the discharge before the current had fully penetrated to the plasma core [9,10] and improved core confinement was also reported in Tore Supra when lower hybrid waves were used to drive current (LHCD) and generate a region of negative magnetic shear in what was called the LHEP mode [11]. In fact, ITBs have been observed in a wide variety of tokamaks and comprehensive reviews have been published [12,13].

Although there is some variety in the observed ITB behaviour, some key features emerge. ITB formation is often favoured by weak or negative magnetic shear, which can be obtained in several different ways. A typical tokamak plasma has a peaked electron temperature profile, which tends to produce a peaked inductive current density profile, monotonic q-profile and positive magnetic shear. The generation of weak or negative magnetic shear requires a broad or hollow current profile, which can be achieved in three ways: by driving off-axis current non-inductively by neutral beams or waves (as in the LHEP mode); by generating a large bootstrap current, which is driven in an off-axis location by the plasma pressure gradient (as in the PEP mode); or by ramping the plasma current, which adds current density transiently in the plasma periphery due to the partially frozen magnetic field (as in the DIII-D and TFTR experiments mentioned above).

Many tokamak observations are consistent with the interpretation that, without an ITB, core plasma transport processes are dominated by turbulence, the effect of which can be suppressed either by reducing the instability growth rate or increasing, for example, the stabilising shear in the E×B flow. Other factors that are thought to affect the stabilisation of turbulence include self-generated zonal flows, the Shafranov shift of adjacent flux surfaces, the ratio of plasma ion and electron temperatures and the presence of impurities. As already noted above, low order rational q surfaces are also seen to play a role in some experiments. These elements are discussed in greater detail in the review articles indicated above and the references found therein. An example of an ITB plasma is shown in figure 1(b) from JT-60U, where the barrier location is indicated by the steep gradient region in the temperature and density profiles. In this case the q-profile shows an associated region of negative magnetic shear in the plasma core.

The aim of this paper is to note some key issues concerning the use of ITBs in the pursuit of steady state tokamak power plant conditions, and highlight a few recent experimental results that

directly address them. It follows from the considerations above that ITB regimes with high H_H must also be capable of stable operation at high β_N if their full potential is to be realised. The plasma pressure profile has a strong influence on the achievable β_N in these regimes, and it has been observed that increasing the pressure profile peaking can lead to a reduction in the achievable value of β_N [14,15,16,17]. Consequently, it is desirable to avoid excessive pressure profile peaking in ITB plasmas by, for example, locating the transport barrier so that it encloses a large fraction of the plasma volume. Aspects influencing the ITB location will be discussed in section 2. The influence of the magnetic topology on the confinement and stability requires that it be sustainable, consistent with the ITB, in steady state. This is particularly challenging when the bootstrap fraction is large and, being driven by gradients in the plasma pressure, can significantly modify the magnetic shear. This is the subject of section 3. In section 4 the issue of maintaining fuel purity against impurity accumulation in the presence of ITBs is discussed. Finally, some conclusions are drawn.

2. OPTIMISATION OF THE ITB LOCATION

No single ingredient determines the location of all ITBs and, in practice, the position and radial extent of a transport barrier depends on the means by which turbulent transport was reduced. The E×B shearing rate is thought to be an important mechanism and can be driven by external momentum input, by tangential NBI, for example, or by pressure gradients in the plasma. Experiments to vary the NBI momentum input by using different beam angles with respect to the plasma have demonstrated a significant effect on ITB dynamics. On TFTR the ITB back transition was hastened using co-injected beams (in the same direction as the plasma current) compared with balanced NBI (similar power from co-injected and counter-injected beams) at the same total heating power level [18]. ITBs in JT-60U were degraded and recovered by varying the toroidal momentum input [19]. Experiments at DIII-D using counter-injected beams resulted in the production of an ITB at larger radius ($\rho \approx 0.7$, where ρ is the normalised minor radius) compared with similar co-injected beams ($\rho \approx 0.5$) [20,21]. In addition to changes in power deposition, due to orbit effects, q-profile evolution, due to the beam driven current direction, and impurity levels in the plasma periphery, it was argued that an interplay between the pressure and toroidal rotation driven terms in the E×B shearing rate could play a role. In the comparison of co-injection versus counter-injection the shearing rate term due to toroidal rotation was essentially reversed while the pressure gradient term was not, modifying the net shearing rate profile and, thus, the ITB location.

A recent comparison of co-injection and counter-injection NBI experiments on MAST, a spherical tokamak, has also revealed differences in the ITB behaviour [22], as illustrated in figure 2. For co-injection the ITB was clearest on the ion heat channel whereas for counter-injection the electron ITB was most evident. The location of the ITB, as indicated by local minima in the energy transport coefficients, appeared at larger normalised minor radius in the counter-NBI case, in line with the DIII-D result, and the density profile was more peaked.

Externally driven flow shear by NBI is clearly an effective means to modify the plasma transport and ITB behaviour in present tokamaks. However, it is not obvious to what extent this experience can be extrapolated to large, high Q devices where achieving high momentum input is more difficult due to the high beam energies required for penetration to the plasma core. This is because, in general, the beam stopping cross-section and the ratio of momentum to energy both decline for beam particles with increasing velocity. Other factors that can affect turbulence stabilisation, such as the introduction of impurities, have also been used to influence ITB dynamics. The introduction of controlled quantities of neon on DIII-D has successfully been used to expand ITBs with co-injected NBI to $\rho \approx 0.7$ and reduce transport as far out as $\rho \approx 0.8$ [21]. ITBs have been generated at high density in Alcator C-Mod with off-axis ICRH [23]. In these experiments the location of the ITB, seen most clearly in the density profile, was expanded by lowering the toroidal magnetic field strength.

Links between ITB dynamics and the shape of the current or q-profile in many experiments suggest this as a candidate mechanism for ITB control. Current profile control has the significant benefit that current drive techniques can be used to tailor the q-profile locally. It is more difficult to envisage such control in the case of other factors affecting turbulence stabilisation such as the Shafranov shift or the ion and electron temperature ratio. Experiments employing plasmas with a region of negative magnetic shear in the core sometimes observe a coincidence between the location of an ITB and the extent of the $s < 0$ region, such that the outer edge, or foot-point, of the ITB is close to the position of $s = 0$. Tailoring the q-profile so as to generate a region of negative magnetic shear could, therefore, provide a means to control the ITB.

At TCV such current profile control has been provided by co-injected electron cyclotron current drive (ECCD), combined with on-axis electron cyclotron heating (ECH). In this case the ability to control the ECCD deposition radius directly was used to scan the current drive location in a series of pulses from the plasma axis to nearly $\rho = 0.5$ [24]. The pulses were fully non-inductive with the pressure driven bootstrap current providing the balance. Figure 3 shows the relative contributions of the ECCD and bootstrap current to the total plasma current as a function of radius of deposition for the ECCD (ρ_{co}). The ECCD efficiency is reduced for off-axis radii due to the lower electron temperature. The strength of the ITB is expressed by ρ^*_T, which is the ratio of the ion Larmor radius at the sound speed and the local temperature gradient scale length [25]. It can be seen from figure 3 that $\rho_{co} > 0.3$ was required to obtain an ITB, and that the ITB location (ρ_{ρ^*}) and strength (ρ^*_{max}) both increased with ECCD deposition radius. In this regime control parameters were identified for both strength and radius of the ITB.

The combination of LHCD and ECH have been used to generate electron ITBs at high plasma density in FTU [26]. The LHCD provided off-axis current drive to generate or maintain a region of low or negative magnetic shear while ECH was used to either heat inside the ITB or to assist the LHCD with off-axis resonance. ITBs have been maintained with a central electron density of $\approx 0.8\times10^{20}$ m^{-3} for over 35 energy confinement times in these experiments. The radius of the ITB was seen to reduce with increasing edge q, which was attributed to an inward shift of the LHCD deposition.

It was noted on DIII-D, however, that the achievement of s = 0 at large radius by tailoring the current ramp up phase of a discharge does not necessarily lead to ITB formation at that location, and experiments that succeeded in generating s = 0 at $\rho \approx 0.9$ exhibited an ITB at $\rho \approx 0.4$-0.5 [21]. Experiments on JT-60U showed that large radius ITBs were obtained ($\rho \approx 0.6$) close to the s = 0 point if they were triggered at an early phase of the current ramp, whereas ITBs formed at later time appeared nearer the plasma centre and far inside the s = 0 location [27]. Thus it can be seen that the achievement of a large region of negative magnetic shear is not always a sufficient condition for the formation of an ITB at large radius.

Experiments have been performed that demonstrate the possibility to expand ITBs after they have been established. On ASDEX Upgrade it was also found that increasing the heating power after a strong transport barrier was formed could result in an increase in the radius of minimum q (q_{min}) and expansion of the ITB [28]. Experimenters on JT-60U have reported a tendency for the outward expansion of strong ITBs in the negative magnetic shear region to be limited to the s = 0 radius unless the temperature gradient was reduced [19]. However, attempts to expand ITBs on JT-60U by increasing the radius of the s = 0 location after barrier formation using LHCD have been successful [29]. An NBI heated plasma was established with negative central shear and an ITB with the foot point near the q_{min} location at $\rho \approx 0.65$. Both negative ion NBI and LHCD were applied to drive current, the LHCD spectrum being chosen to enhance the off-axis current drive. The foot point of the ITB expanded to $\rho \approx 0.75$ following the location of q_{min}, the movement of which was believed to be due to the LHCD. On JET the application of LHCD has extended the duration of ITBs at large radius [30]. In this case the LHCD waves were thought to drive current at the ITB location, thus modifying the evolution of the magnetic shear locally.

Large radius ITB have been generated in JET using either a monotonic q-profile or triggering the barrier at or outside the s = 0 radius in the case of plasmas with negative central magnetic shear. Such ITBs can be triggered either by applying heating in a reversed shear configuration early in the discharge while q_{min} is high (above 2 or 3), in which case an ITB can be triggered as q_{min} falls to reach an integer value [31]. Such effects have been seen on other devices [e.g. 32]. Alternatively, an ITB trigger can be achieved at a q=integer surface in the positive shear region if sufficient heating is applied during the current ramp at a time when the value of q near the edge of the plasma reaches an integer value. In this case it is thought that an MHD instability associated with a q = integer surface near the plasma edge may couple with the interior q = integer surface to locally modify the plasma flow shear, and hence trigger an ITB [33]. In this case some control can be achieved over the starting location of the barrier [34]. Transport barriers have also been obtained at large radius in JT-60U in the positive magnetic shear region of high-β_p mode plasmas, in which they have also been associated with integer q-surfaces [8].

Figure 4 shows the radial location at which a strong ion ITB was initially diagnosed in high magnetic field strength (3.3-3.6T) JET plasmas without significant LHCD preheat (i.e. mainly monotonic target q-profiles). The barrier radii have been plotted against the additional heating

power required to achieve them. A strong ITB is defined here as one for which $\rho^*_{Ti} > 0.021$, which is 50% higher than the empirical threshold for an ITB on JET [25]. The use of this strong ITB definition, together with the limited temporal and spatial resolution of the large dataset used in this analysis, means that the figure represents the access conditions for substantial confinement improvement rather than the threshold conditions for ITB formation. ITBs can be obtained at lower power, but tend to remain weak. It can be seen from figure 4 that the minimum power required to form a strong ITB increases with the radius. However, once generated, strong ITBs can expand to larger radius without a further increase in heating power, as shown in the same figure. This is consistent with the picture that an increase in flow shear, due to transport reduction, and a reduction in magnetic shear, due to the bootstrap current and current pile up, can allow the ITB to expand [35]. This suggests that expanding core ITBs may be more efficient than triggering ITBs directly at large radius and relatively high magnetic shear.

JET plasmas with weakly negative central magnetic shear can generate weak core ion ITBs when heated strongly. One such case is illustrated in figure 5, which shows the q-profile at the start of the main heating phase where a fast current ramp without LHCD had been used. Main heating began just as q_{min} fell below 3, so the trigger for an ITB in the positive magnetic shear region was missed. A core ITB was formed and the q-profile developed a region of strongly negative magnetic shear, as seen in figure 5. The current was ramped slowly during the main heating phase, but simulations using the TRANSP code [36], also shown in figure 5, suggest that significant shear reversal could not be explained without non-inductive current drive (NBI and bootstrap), and that the bootstrap effect was the dominant term. The increasing strength of the ITB is consistent with a transport reduction due to the stronger shear reversal, although the plasma flow shear and Shafranov shift also increases due to the improved core confinement, which may have reinforced this positive feedback process. After 2.8 s the plasma disrupted due to a pressure driven MHD instability as q_{min} approached 2. The total non-inductive current in the TRANSP simulation was about one third of the plasma current. This shows that, in the core region, q-profile runaway to deep shear reversal can occur with relatively small bootstrap current fractions, and highlights the importance of active control for the sustainment of the magnetic topology in ITB plasmas.

In high Q devices further feedback processes can be expected. In particular, the formation or strengthening of an ITB would lead to an increase in α-heating due to the core pressure rise, which, in turn, could further strengthen the barrier. In fact, long pulse experiments on Tore Supra with LHCD have exhibited core temperature oscillations that have been attributed to nonlinear coupling of the current density and electron temperature [37]. In this case it was argued that the q-profile could be modified by the LHCD to provide a core confinement improvement, perhaps in the manner of earlier LHEP experiments [11]. The consequent increase in core temperature would then modify the efficiency and profile of the LH driven current so as to reverse the original q-profile change and degrade the transport reduction. Such experience emphasises the need for long pulse experiments and real-time control.

Experimenters have been successful in finding means to control the location of ITBs and increase the plasma volume that they enclose. q-profile control probably remains the prime candidate for application to high Q devices, but a distinction has to be made between the plasma initiation phase and the steady state conditions. It is clear that there are particular issues concerning the ITB formation phase, for example: developing the optimum location and strength, avoiding deleterious MHD instabilities during the initial evolution of the q-profile, avoiding uncontrolled runaway scenarios, etc. However, during this transient, low Q phase a relatively large fraction of the plasma heating power and current could be driven by external systems to establish a suitable regime. During steady, high Q operation, the control actuators will be relatively weaker, and it is desirable to find scenarios that only require minor tuning to maintain confinement and stability. ITB control schemes are required to manage both of these circumstances if transport barriers are to be exploited fully in next generation devices.

3. CONTROL AND SUSTAINMENT OF THE ITB AND MAGNETIC TOPOLOGY

Steady plasma scenarios with improved confinement compared with H mode have been developed that rely on avoidance of q = 1 sawtooth instabilities. This appears to be achieved by subtle q-profile modifications, for example due to fishbone instabilities [38,39] or 3/2 tearing modes [40]. These regimes have broad pressure profiles and are capable of stationary high β_N operation, which would be attractive for application to future devices. Sometimes called “improved H mode,, or “hybrid,, regimes, they do not typically exhibit a strong localised ITB and it is unclear if turbulence suppression plays a significant role in the achieved performance in these cases. Nevertheless, these scenarios serve to illustrate that a range of performance enhancement regimes are becoming accessible through manipulation of the q-profile shape.

Plasma scenarios aimed at steady-state operation in future devices, on the other hand, are currently envisaged to have a high bootstrap fraction, and hence are naturally suited to the low or negative magnetic shear requirements of ITB regimes. When ITBs and substantial bootstrap current fractions are involved, feedback control of the pressure and/or current profiles becomes increasingly desirable to achieve and maintain the required conditions.

On DIII-D experiments were conducted with about 2.5 MW of off-axis co-injected ECCD to modify the current density profiles of a plasma with $q_{min} > 2$ [41]. NBI heating was applied during the current ramp up phase and increased at the end of the ramp to be used under feedback control to maintain $\beta_N \approx 2.8$. ECCD was injected at $\rho \approx 0.4$, which resulted in the central value of q rising to nearly 5. The confinement in the negative shear region improved due to a weak transport barrier located near the ECCD deposition radius, as seen in figure 6, and the confinement enhancement factor with respect to the ITER98y2 scaling [2], H_{98y2}, was 1.3. An equivalent pulse with radially launched electron cyclotron heating (ECH), but no current drive, is also shown in figure 6 for comparison. The regime was maintained until the end of the 2s ECCD pulse, which represents several confinement times. The contribution of the inductive current drive is calculated to be only 10 % of the total plasma current with 55 % being provided by the bootstrap effect.

Control of ITB strength has been achieved on JT-60U by varying either the neutral beam power or toroidal momentum input [19]. The beams can provide flow shear directly through toroidal momentum input or indirectly by modifying the pressure gradient, which also generates E×B flow shear. These two contributions can tend to reinforce or cancel each other locally depending on the direction of the beams and the pressure profile shape. Thus variation of the beam configuration and power can influence turbulence stabilisation and ITB behaviour. In an ITB plasma with negative central magnetic shear it was found that the switch from balanced to net co-injection was followed by a degradation of the barrier. The power of the JT-60U neutral beams with perpendicular injection angle (no significant toroidal momentum input) increased under feedback control to maintain the diamagnetic stored energy. This led to the recovery of the pressure gradient at the ITB. The sequence of ITB degradation and recovery was repeated twice more during the discharge. Feedback control of the electron temperature gradient in ITB plasmas using the beam heating power has also been developed on JT-60U [42].

Multi-variable real-time control schemes have been developed on JET [43]. Feedback control of the ITB strength has been employed using ion temperature [44] or electron temperature gradients [45]. Combined control of neutron yield using NBI power and normalised electron temperature gradient using ICRH power has allowed weak ITBs to be maintained in more steady conditions than with pre-programmed power waveforms. Real-time q-profile control has also been developed at JET [43] using polarimetric measurements. Figure 7 shows an example where 3 actuators were employed (LHCD, ICRH and NBI). When the feedback control was activated at t = 7 s the q-profile had a large region of negative magnetic shear, compared with the weak shear reference, and the initial off-axis current was still diffusing inwards. At t = 11 s the q-profile was close to the requested shape and the actuators began to act against further diffusion. A modelling calculation of the current density profiles for the LHCD and NBI, as well as the bootstrap current, are also shown in figure 7. The ICRH waves did not drive any significant current directly, but acted on the q-profile through the bootstrap current, together with the other heating systems. It can be seen that the LHCD and NBI systems drove current at quite different radial locations, providing a degree of control over the q-profile shape. The control matrix was determined in this case using reference pulses in which the response of the plasma to a power step-down was evaluated for each actuator in turn.

Whereas the influence of actuators on the pressure and q-profile may be quite significant while the plasma scenario is being established in a high Q device, it would, in general, be highly advantageous if the pressure driven bootstrap current were well aligned with the total current density profile. Experiments on TCV have succeeded in maintaining an ITB plasma in steady-state with 70 – 80 % of the current provided by the bootstrap mechanism [46]. The plasma was initially heated with central ECH and then a further two EC beams were added: one off-axis ECH and one on-axis counter-ECCD, reaching a total power of 2.2 MW. An electron ITB was evident on the temperature and weakly on the density profiles, and was maintained at a constant radius (within diagnostic resolution) for 600 ms, which corresponds to 300 energy confinement times and 4 current

redistribution times. The q-profile was believed to be non-monotonic due to the large bootstrap fraction and demonstrates the potential for good alignment between ITB generated bootstrap current and the q-profile required to sustain an ITB.

Sustainment of ITB plasmas with high confinement and high bootstrap current fraction has been achieved in JT-60U [47]. Figure 1 shows the time evolution of such a discharge. An ITB is evident on the temperature and density profiles where the 'foot' of the steep gradient region is at $\rho \approx 0.7$. The magnetic shear is negative in the plasma core and the $s = 0$ point is at $\rho \approx 0.65$. The current is believed to be fully non-inductive with about 80 % being driven by the bootstrap mechanism. q_{95} was about 9 in the high performance phase of this discharge and the confinement exceeded the ITER98y2 scaling by a factor ≈ 2.2 and the ITER89L-P L mode scaling [48] by ≈ 3.5. This, and a normalised β value of ≈ 2, were sustained for 2.7 s (about 6 energy confinement times). Figure 1 also shows that the density and q-profiles were almost stationary during this high performance phase. In fact, in a series of such discharges in JT-60U the shrinkage of the radius of $s = 0$ was observed when β_P (and hence the bootstrap fraction) was small, and sustainment of $s = 0$ at large radius was only achieved at high β_P.

The development of real-time control techniques and the identification of regimes with a high degree of bootstrap current alignment are highly advantageous for the sustainment of the magnetic topology in ITB plasmas. The demonstration of such capabilities at even higher β_N are required if the full potential of ITB plasmas is to be realised for future applications.

4. FUELLING AND IMPURITY CONTROL

In addition to the achievement of confinement improvement compared with the ELMy H-mode and stability compatible with high β_N in steady conditions, it is necessary to maintain a high degree of plasma fuel purity to facilitate efficient operation at high Q. Many present tokamak experiments provide significant core fuelling using NBI, but this is energetically unfavourable for an ITER sized tokamak. In such a case beam energies of order 1MeV are required to achieve central deposition at densities approaching the Greenwald value ($n_{GR} = I_{MA}/\pi a^2$ where n_{GR} has units 10^{20} m^{-3} [49]), which are required for high fusion yield. With each deuteron and triton pair injected at a cost of 2 MeV and fused to generate 17.6 MeV, an additional source of fuel would be required to achieve high Q, even in the unrealistic case that every beam particle fused before leaving the plasma.

Combined pellet injection and additional heating has provided a means to generate high performance core fuelled plasmas with or without NBI [7,50,51,52,53,54,55]. In early JET experiments it was believed that the q-profile was strongly modified by the bootstrap current generated by the pellet induced density peaking, thus there was only limited prospect for control of the magnetic topology. More recent experiments [56] have demonstrated that a region of negative central magnetic shear could be maintained while a stream of small pellets were injected at low velocity ($\approx$ 80 m/s) on the high field side of the plasma in the presence of low power NBI heating. In these experiments a hollow current profile was generated using LHCD during the initial phase of

the current ramp, during which time a core electron ITB was observed. The LHCD was then switched off and a 1 s 'gap' was used for pellet fuelling and low power (about 4MW) NBI before main NBI and ICRH heating was applied. Figure 8 shows an example of the increase in core density achieved by this technique. The measured q-profile is also shown after the first and fourth pellets in this pulse to illustrate the preservation of the region of strongly negative magnetic shear in the plasma core. The addition of the NBI during the pellet 'gap' is believed to inhibit the current diffusion by increasing the temperature while not heating the plasma sufficiently to inhibit good pellet penetration. In this scenario ITBs were triggered with 15 MW of main heating after the 'gap', but only in cases with both LHCD and pellets [56]. Initial attempts to refuel such plasmas during main heating showed that pellet deposition outside a strong ITB could modify the plasma edge conditions without affecting the barrier, while deeper penetration could cause a reduction in the temperature gradient or destruction of the ITB [57]. These experiments suggest the potential application of pellet injection to next generation devices as a means to establish high density ITBs, modify plasma edge conditions for divertor compatibility or interrupt ITBs. The ability to sustain ITBs in high density plasmas with reversed magnetic shear has been demonstrated in FTU experiments (mentioned earlier) [26]. The issue of plasma purity is of particular importance in ITB scenarios due to the observation of impurity particle transport modification in many current experiments. A detailed study has been made for different ITB regimes on JT-60U [58] showing accumulation of argon inside the barrier, but not helium or carbon. A correlation was found between the electron diffusivity and ion thermal diffusivity at the barrier, and the steep density gradients generated in the case of strong ITBs were considered to play an important role in the argon transport through the neoclassical inward convection velocity. A clear difference was found between ITBs generated in plasmas with reversed shear and the positive magnetic shear high β_p mode. The ion thermal transport of high performance ITBs in the negative shear regime approached the neoclassical level, whereas in the high β_P mode the transport remained well above the neoclassical level, although an ITB was observed. The density gradient was typically steeper for strong ITBs in the reversed shear regime, called 'box-type' due to the extreme profile shapes, which correlated with a stronger peaking of the argon density profile. In JET impurity behaviour in ITB plasmas has also been studied for ITBs in both negative and positive magnetic shear plasmas. Comparison of strong ITBs with strongly peaked electron density profiles exhibited metallic impurity accumulation in both cases [59]. The density peaking increased with impurity charge, consistent with expectations based on neoclassical transport. Experiments have been performed to compare the impurity behaviour of weak and strong ITBs in a positive magnetic shear regime on JET using a laser blow off technique to seed nickel impurities in the plasma edge [60]. The observations showed that the nickel levels decayed much more quickly in the case of the weak ITB, which also exhibited a less peaked electron density profile.

A link between density peaking and impurity accumulation is particularly relevant to ITB experiments on present devices using NBI, which provides effective core fuelling. Experience of peaked density profiles in plasmas without an ITB has shown from long ago that the addition of

core radio frequency heating can sometimes reduce the density peaking. Carefully controlled investigations have been performed on ASDEX Upgrade using NBI heated, high density ELMy H mode plasmas where density peaking occurs slowly during a phase of strong gas puffing [61]. Replacing some of the NBI heating with ICRH to increase the peaking of the heat deposition profile resulted in a reduction in the density peaking. In fact, adding the ICRH to the NBI to maintain the beam fuelling rate had the same effect. The proposed interpretation was that the increased central heating increased the turbulent transport and thus degraded the particle transport [62]. Density profile flattening has also been observed on several devices when ECH is applied centrally in plasmas where turbulent transport is dominant (see [62] and references therein). Given the picture that ITBs are formed by the reduction or practical elimination of the turbulent transport, it is not immediately evident that such methods for particle transport control would be applicable to ITB plasmas.

The ITBs generated using off-axis ICRH in Alcator C-Mod (mentioned earlier) have also exhibited density peaking and an associated impurity peaking [23]. This rise in density and impurities could be arrested by adding on-axis ICRH, even though the density peaking was considered to be due to an ITB in this case. At DIII-D, a quiescent H-mode has been combined with a weak ITB to generate quiescent double barrier (QDB) plasmas. In this regime the addition of 2 MW of ECH or ECCD in the core of plasmas with an established barrier substantially broadened the density profile [63], as shown in figure 9, and the density profile of high Z impurities was effectively flattened. The effect was sensitive to the EC resonance location, with a weaker effect for EC deposition at $\rho \approx 0.4$. It is interesting to note that the core barrier in DIII-D QDB plasmas is attributed to a reduction in the turbulence correlation length rather than a complete suppression of turbulence [64].

In JT-60U the effect of core electron heating on particle transport was investigated for ITB plasmas in both the reversed shear and high β_P mode regimes described above [58]. It was found that the density peaking was reduced and argon exhausted by applying ECH to weak ITBs in the high β_P mode regime, but not for strong box-type ITBs in reversed shear plasmas. It has also been reported that the ion temperature gradient at the ITB in JT-60U is degraded by dominant electron heating in the case of the high β_P mode, whereas clear ITBs are maintained in the reversed shear scenarios [65].

Density gradients appear to be efficient at driving both high Z impurity accumulation and bootstrap current. The optimisation of the density profile represents, therefore, an important issue for prospective steady state regimes for ITER and power plants. The observations of the sensitivity of particle transport to central electron heating in cases where turbulence suppression is incomplete, suggests a potential route for such optimisation. Experiments are required to further explore high performance regimes with improved core confinement in the domain of dominant electron heating to build on present investigations.

CONCLUSIONS

A range of confinement improvement regimes has emerged in present experiments covering standard H mode, improved H mode (or hybrid scenarios), and a variety of weak and strong ITBs. Whereas strong ITBs with essentially complete suppression of turbulent transport have highly attractive

energy confinement, the challenges in terms of stability as well as fuel and impurity transport are considerable. Regimes whose transport is characterised by incomplete suppression of turbulent transport are being developed with many of the features required for compatibility with future use in high Q devices, and it appears that the currently envisaged parameters for the non-inductive operation of ITER represent realistic first target for such scenarios [1]. Access to high values of β_N (≥ 3) remains highly desirable for high fusion yield and the high bootstrap fraction required for Advanced Tokamak scenarios, and creative approaches to plasma stability would be required, perhaps including conducting walls or feedback controlled external coils. Finally, the compatibility with the safe operation of the divertor on future machines is essential for all plasma scenarios being validated for high Q applications. ITB plasmas have been obtained with a wide range of plasma edge conditions, but have also demonstrated a sensitivity to particular features, such as ELMs. This, together with the above considerations emphasises the need for integrated validation of candidate plasma regimes for steady state high Q operation, including the use of power plant relevant heating and fuelling.

ACKNOWLEDGEMENTS

It is a pleasure to acknowledge the help of Dr Yu Baranov and Dr N C Hawkes with the TRANSP and MSE analysis of the data in figure 5, Dr J Mailloux for assistance with database used to generate figure 4 and the contributors to the EFDA-JET workprogramme [66] for the use of JET data. Some of the data presented was produced within the framework of the JET Joint Undertaking. Also many thanks to Dr Burrell, Dr Fujita, Dr Henderson, Dr Joffrin, Dr Meyer, Dr Moreau and Dr Wade for their kind permission to include figures from their work. This work was funded partly by the United Kingdom Engineering and Physical Sciences Research Council and by EURATOM.

REFERENCES

[1]. Green B.J. *et al.,* 2003 *Plasma Phys Control Fusion* **45** 687
[2]. ITER Physics Basis 1999 *Nuclear Fusion* **39** 2137
[3]. Rebut P-H, Boucher D, Gormezano C, Keen B.E, and Watkins M.L, 1993 *Plasma Phys. Control. Fusion* **35** A3
[4]. Cordey J.G, Challis C.D and Stubberfield P.M, 1988 *Plasma Phys. Control. Fusion* **30** 1625
[5]. Kikuchi M. 1990 *Nuclear Fusion* **30** 265
[6]. Najmabadi F. *et al.,* 1997 *Fusion Eng. Des.* **38** 3
[7]. Hugon M. *et al.,* 1992 *Nuclear Fusion* **32** 33
[8]. Koide Y. *et al.,* 1994 *Phys. Rev. Lett.* **72** 3662
[9]. Levinton F.M, *et al.,* 1995 *Phys. Rev. Lett.* **75** 4417
[10]. Strait E J *et al.,* 1995 *Phys. Rev. Lett.* **75** 4421
[11]. Litaudon X. *et al.,* 1996 *Plasma Phys. Control. Fusion* **38** A251

[12]. Wolf R.C, 2003 *Plasma Phys. Control. Fusion* **45** R1
[13]. Connor J.W, *et al.,* 2004 *Nuclear Fusion* **44** R1
[14]. Chu M.S, *et al.,* 1996 *Phys. Rev. Lett.* **77** 2710
[15]. Huysmans G.T.A, *et al* 1999 *Nuclear Fusion* **39** 1489
[16]. Kikuchi M, *et al* 2001 *Plasma Phys. Control. Fusion* **43** 217
[17]. Challis C.D, *et al* 2002 *Plasma Phys. Control. Fusion* **44** 1031 (Erratum 2002 *Plasma Phys. Control. Fusion* **44** 2063)
[18]. Synakowski E.J, *et al.,* 1997 *Phys. Rev. Lett.* **78** 2972
[19]. Sakamoto Y, *et al.,* 2001 *Nuclear Fusion* **41** 865
[20]. Greenfield C.M, *et al.,* 2000 *Phys. Plasmas* **7** 1959
[21]. Doyle E.J, *et al.,* 2002 *Nuclear Fusion* **42** 333
[22]. Meyer H, *et al.,* 2004 *Plasma Phys. Control. Fusion* **46** A291
[23]. Rice J.E, *et al.,* 2003 *Nuclear Fusion* **43** 781
[24]. Henderson M.A, *et al.,* 2004 *Plasma Phys. Control. Fusion* **46** A275
[25]. Tresset G, *et al.,* 2002 *Nuclear Fusion* **42** 520
[26]. Pericoli Ridolfini V, *et al.,* 2003 *Nuclear Fusion* **43** 469
[27]. Fujita T, *et al.,* 1999 *Nuclear Fusion* **39** 1627
[28]. Wolf R.C, *et al.,* 2001 *Nuclear Fusion* **41** 1259
[29]. Ide S, *et al.,* 2002 *Plasma Phys. Control. Fusion* **44** L63
[30]. Mailloux J, *et al.,* 2002 *Phys. Plasmas* **9** 2156
[31]. Joffrin E, *et al.,* 2003 *Nuclear Fusion* **43** 1167
[32]. Bell M.G, *et al.,* 1999 *Plasma Phys. Control. Fusion* **41** A719
[33]. Joffrin E, Challis C.D, Hender T.C, Howell D.F, Huysmans G.T.A, 2002 *Nuclear Fusion* **42** 235
[34]. Challis C.D, *et al.,* 2001 *Plasma Phys. Control. Fusion* **43** 861
[35]. Parail V.V, *et al.,* 1999 *Nuclear Fusion* **39** 429
[36]. Budny R.V, *et al.,* 1995 *Nuclear Fusion* **35** 1497
[37]. Giruzzi G, *et al.,* 2003 *Phys. Rev. Lett.* **91** 135001-1
[38]. Sips A, Hobirk J and Peeters A.G, 2003 *Fusion Sci. Tech.* **44** 605
[39]. Sips A.C.C, *et al.,* 2003 *Proc. 30th EPS Conf. on Control. Fusion and Plasma Phys. (St. Petersburg, 2003)* vol 27A (ECA) O-1.3A
[40]. Luce T.C, *et al.,* 2003 *Nuclear Fusion* **43** 321
[41]. Wade M.R, *et al.,* 2003 *Nuclear Fusion* **43** 634
[42]. Oikawa T, *et al.,* 2000 *Nuclear Fusion* **40** 1125
[43]. Moreau D *et al.,* 2003 *Nuclear Fusion* **43** 870
[44]. Joffrin E, *et al.,* 2003 *Plasma Phys. Control. Fusion* **45** A367
[45]. Mazon D, *et al.,* 2002 *Plasma Phys. Control. Fusion* **44** 1087
[46]. Sauter O, *et al.,* 2003 *Proc. 19th Int. Conf. on Fusion Energy (Lyon, 2002)* (Vienna: IAEA) EX/P5-06

[47]. Fujita T, *et al.,* 2002 *Nuclear Fusion* **42** 180
[48]. Yushmanov P.N, *et al.,* 1990 *Nuclear Fusion* **30** 1999
[49]. Greenwald M, *et al.,* 1988 *Nuclear Fusion* **28** 2199
[90]. Kamada Y, *et al.,* 1991 *Nuclear Fusion* **31** 23
[51]. Geraud A, *et al.,* 1994 *Proc. 21st EPS Conf. on Control. Fusion and Plasma Phys. (Montpellier, 1994)* vol 18B, pt 1 (ECA) p 298
[52]. Takase Y, *et al.,* 1996 *Plasma Phys. Control. Fusion* **38** 2215
[53]. Baylor L.R, *et al.,* 1997 *Nuclear Fusion* **37** 12
[54]. Baylor L.R, *et al.,* 2001 *Proc. 18th Int. Conf. on Fusion Energy (Sorrento, 2000)* (Vienna: IAEA) EXP5/04
[55]. Frigione D, *et al.,* 2001 *Nuclear Fusion **41** 1613*
[56]. Frigione D, *et al.,* 2003 *Proc. 30th EPS Conf. on Control. Fusion and Plasma Phys. (St. Petersburg, 2003)* vol 27A (ECA) P-2.91
[57]. Garzotti L, *et al* this conference
[58]. Takenaga H, *et al.,* 2003 *Nuclear Fusion* **43** 1235
[59]. Dux R, *et al.,* 2004 *Nuclear Fusion* **44** 260
[60]. Chen H, Hawkes N.C, Ingesson L.C, Peacock N.J, and Haines M.G, 2001 *Nucl. Fusion* **41** 31
[61]. Stober J, *et al.,* 2001 *Plasma Phys. Control. Fusion* **43** A39
[62]. Angioni C, *et al.,* 2004 *Nuclear Fusion* **44** 827
[63]. Burrell K.H, *et al.,* 2003 *Nuclear Fusion* **43** 1555
[64]. Doyle E.J, *et al.,* 2001 *Plasma Phys. Control. Fusion* **43** A95
[65]. Ide. S, *et al.,* 2004 *Nuclear Fusion* **44** 87
[66]. Pamela. J, *et al.,* 2003 *Proc. 19th Int. Conf. on Fusion Energy (Lyon, 2002)* (Vienna: IAEA) OV/1-4

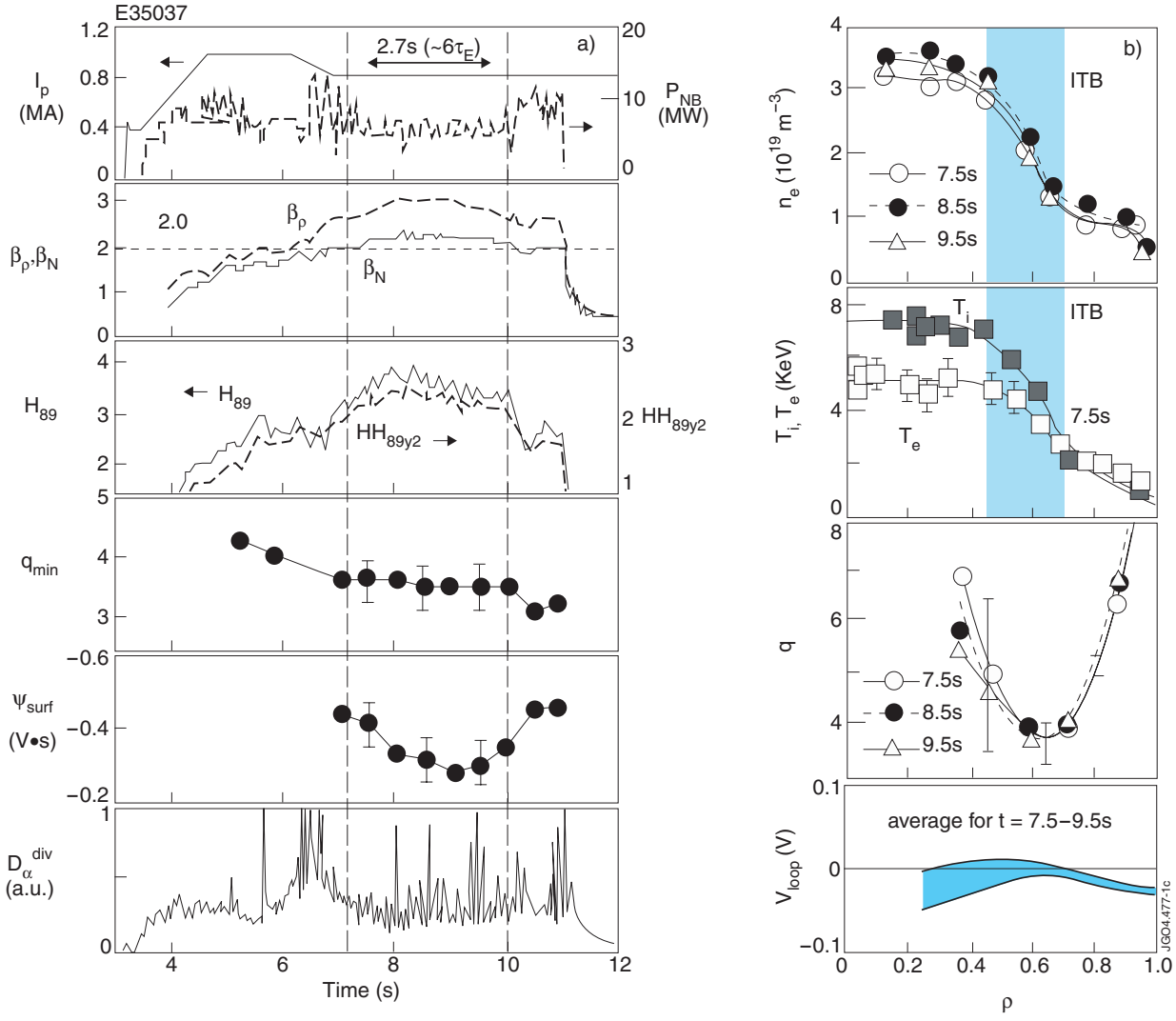

Figure 1: High confinement ITB maintained with bootstrap current fraction on JT-60U. Time traces (a) show the plasma current, NBI power, β_P, β_N, H_{89} (confinement enhancement compared with ITER89L-P L mode scaling), H_{H98y2}, q_{min} (minimum value of q), ψ_{surf} (surface flux), and D_α (deuterium recycling emission at the divertor). (b) shows the electron density, electron and ion temperature, q and loop voltage profiles from t = 7.5 – 9.5 s. (reproduced from [47])

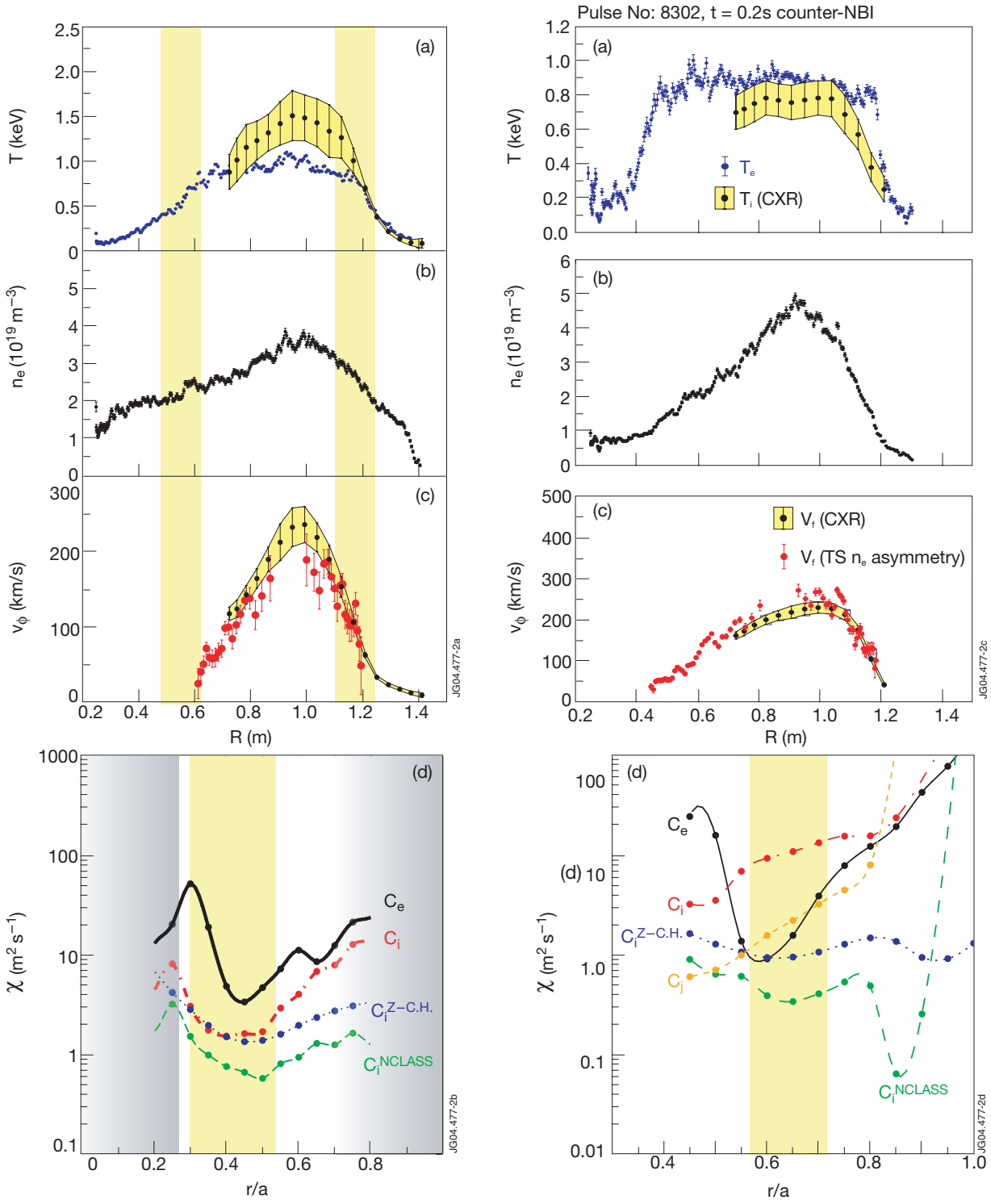

Figure 2: Comparison of ITB behaviour in MAST for co-injected (#8575) and counter-injected (#8302) NBI. Shown are the (a) electron and ion temperature, (b) electron density and (c) toroidal rotation profiles. The rotation velocity was evaluated from Charge Exchange Recombination (CXR) measurements and the asymmetry in Thomson scattering density measurements. Energy transport coefficients (d) are shown compared with neoclassical calculations using NCLASS and following Chang and Hinton (with Z_{eff} correction). The toroidal ion momentum diffusion coefficient is also show in the counter-NBI case. The ITB region is shaded. (reproduced from [22])

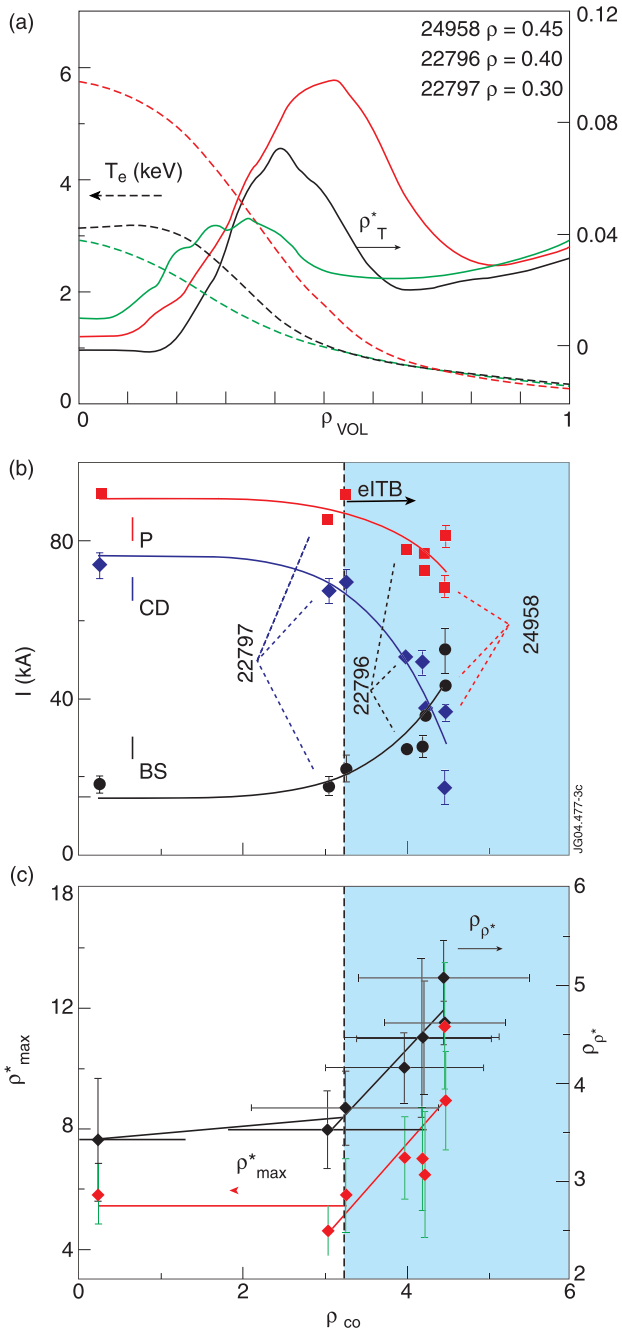

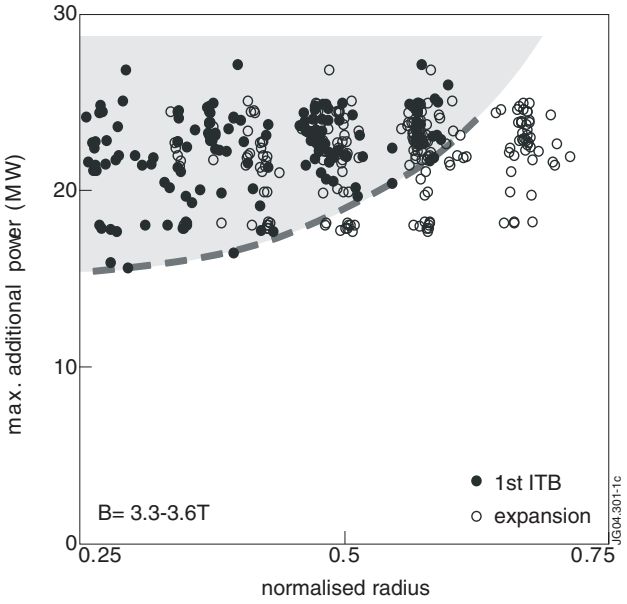

Figure 3: Variation of ECCD (I_{CD}), bootstrap current (I_{BS}), electron ITB strength (ρ^*_{max}) and location (ρ_{ρ^*}) with co-ECCD deposition location (ρ_{co}) in TCV. Also shown are example electron temperature and ρ^*_T profiles from the scan (reproduced from [24])

Figure 4: Radial location of strong ion ITBs plotted against heating power required to achieve them in the JET positive shear regime at high magnetic field. Solid symbols show the initial observation of the strong ITB, limited to the shaded region, and open symbols indicate the subsequent barrier expansion.

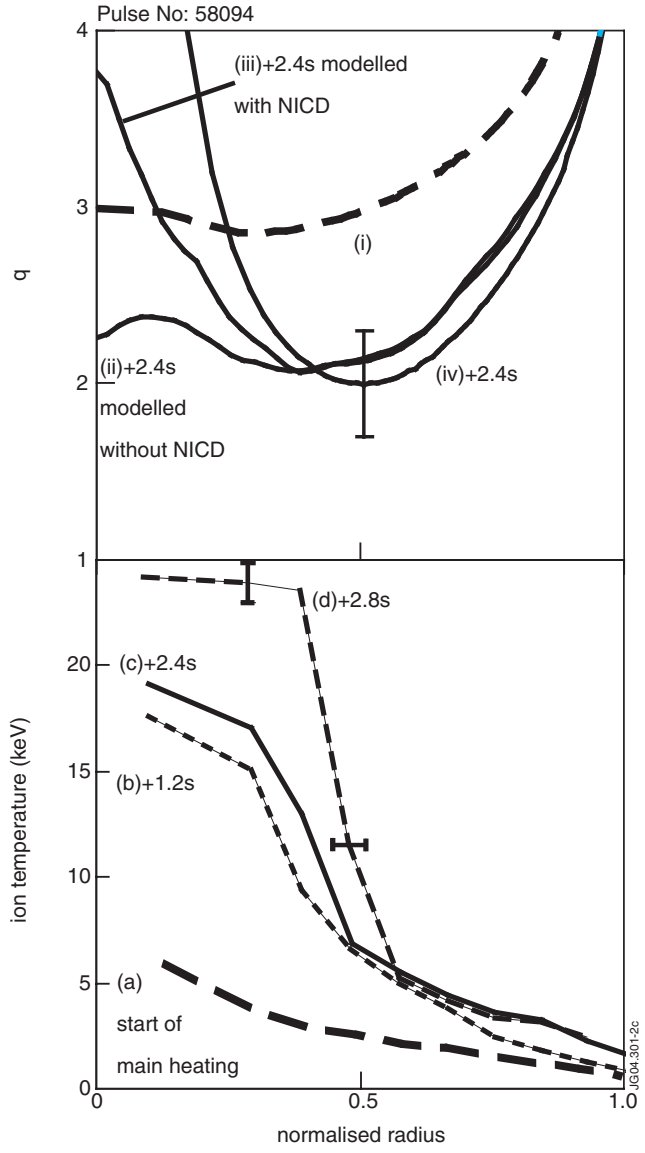

Figure 5: Initial ion temperature (a) and q-profile (i) at the start of main heating in JET. Ion temperatures show a core ITB with increasing strength during main heating (b-d), generating magnetic shear reversal as seen from the q-profile evaluated using motional stark effect measurements (iv). TRANSP simulations with (iii) and without (ii) non-inductive current drive (NICD) confirm the role of bootstrap and beam driven currents.

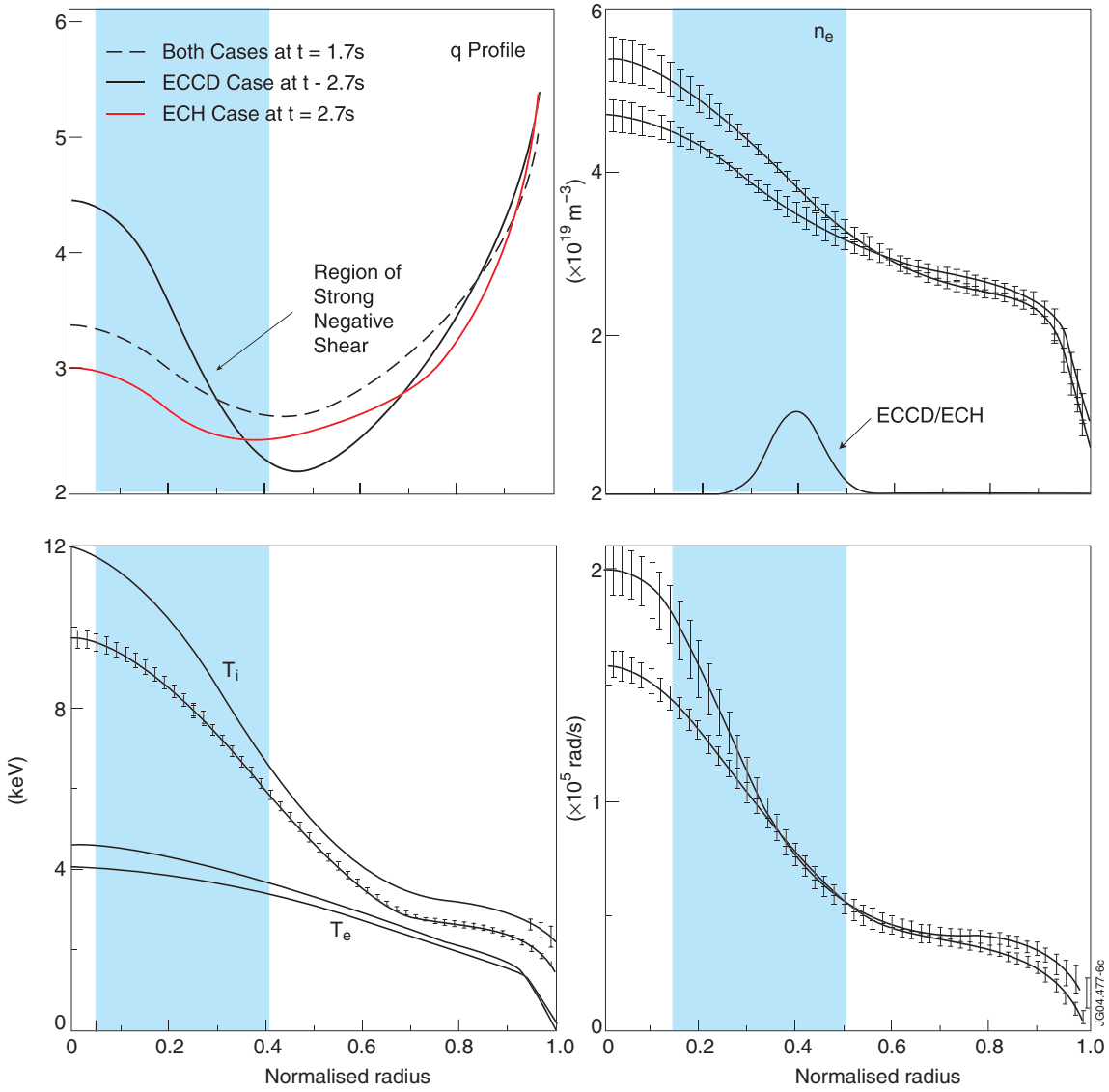

Figure 6: Profiles of q, electron density (n_e), ion temperature (T_i), electron temperature (T_e) and toroidal rotation (Ω_{tor}) in pulses with ECCD (light) and ECH (dark). Also show is the deposition location of the ECCD/ECH and a q-profile representing the start of the EC phase in both pulses (dashed). (reproduced from [41])

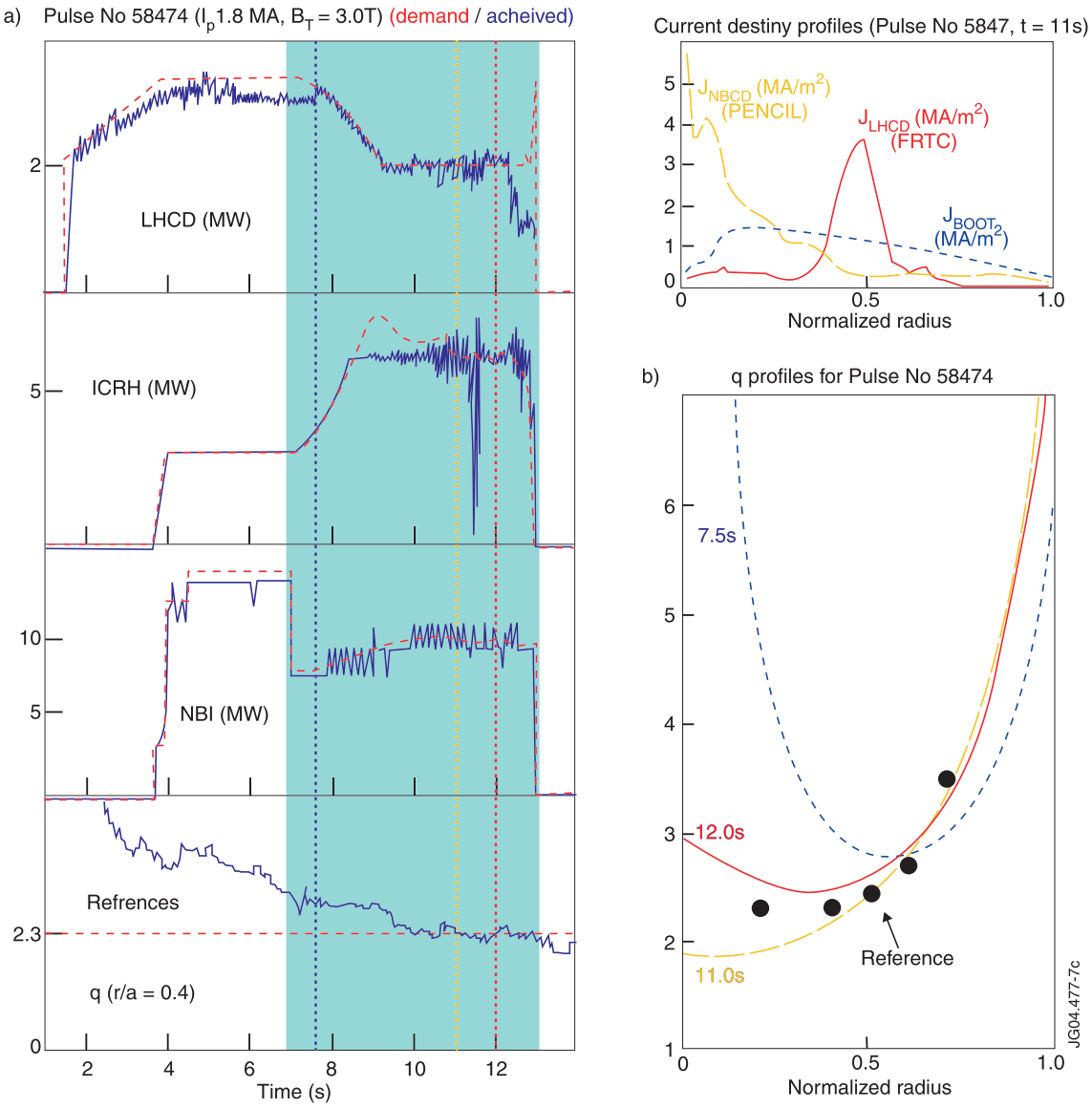

Figure 7: Real-time q-profile shape control using 3 actuators on JET. Power from LHCD, ICRH and NBI are shown in (a) together with q at r/a = 0.4, determined in real-time. The period when control was active is also shown, and the measured q-profile at 3 times (b) along with the reference points. The calculated current density profiles for NBCD, LHCD and bootstrap current are shown at t = 11 s. (reproduced from [44])

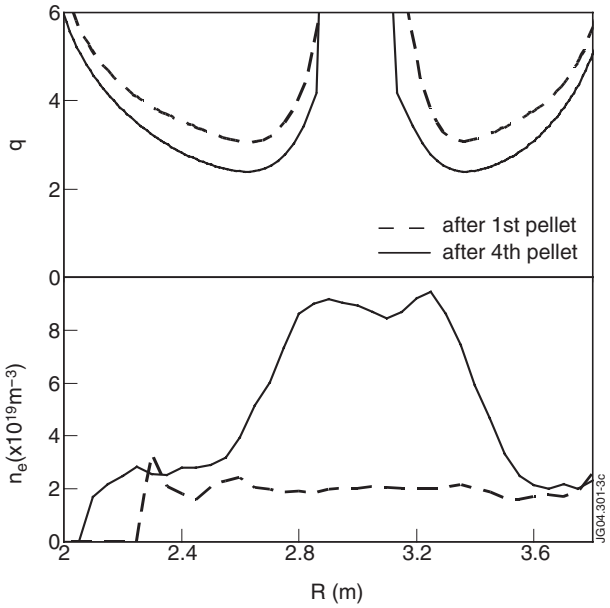

Figure 8: q-profile (measured using MSE) at t = 3.3 s (after the first pellet) and t = 4.0 s (after the fourth pellet) following an LHCD preheat, which generated strongly reversed magnetic shear. 3.9MW of NBI was applied during t = 3 – 4 s. Also shown is the density build up due to the pellet fuelling, illustrated at t = 3.38s (after the first pellet) and t = 4.13s (after the fourth pellet).

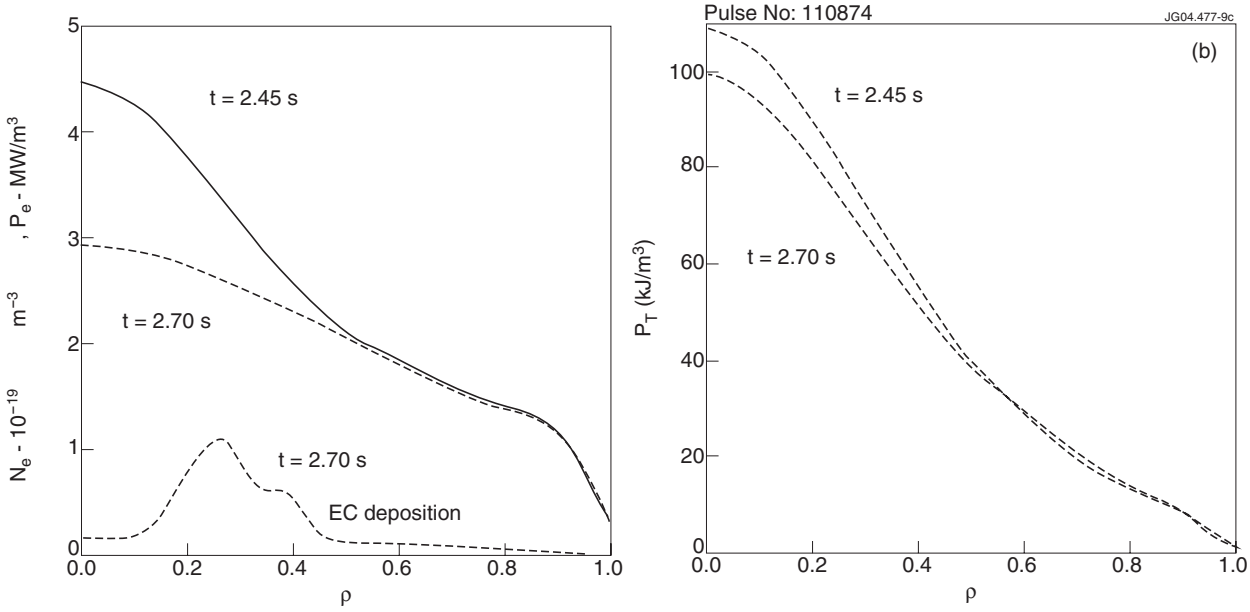

Figure 9: (a) electron density profiles and (b) total pressure profiles in QDB plasmas in DIII-D with (dashed lines) and without (solid lines) ECH. The calculated EC deposition profile is also shown. (reproduced from [63])